



## **FABRICATION OF SENSOR PACKAGES ENABLED BY ADDITIVE MANUFACTURING**

**= Deliverable D4.1 =**

**Prototype of Inspection Equipment**



This project has received funding from the European Union's Horizon 2020 research and innovation programme under the Grant agreement n°958472, project TINKER.



*DT-FOF-07-2020*  
*Assembly of micro parts (RIA)*

# **TINKER**

## **FABRICATION OF SENSOR PACKAGES ENABLED BY ADDITIVE MANUFACTURING**

Starting date of the project: 01/10/2020  
Duration: 36 months

---

### **= Deliverable D4.1 =** **Prototype of Inspection Equipment**

Due date of deliverable: 30/06/2021  
Actual submission date: 25/06/2021

Responsible WP: Sebastian Zambal, WP4, PRO  
Responsible TL: Robert Meyer, SEN  
Revision: V1.3

## TINKER

## AUTHOR

Author	Institution	Contact (e-mail, phone)
Sebastian Zambal	PRO	<a href="mailto:sebastian.zambal@profactor.at">sebastian.zambal@profactor.at</a>
Robert Meyer	SEN	<a href="mailto:robert.meyer@sentech.de">robert.meyer@sentech.de</a>

## DOCUMENT CONTROL

Document version	Date	Change
V1.0	20.05.2021	Template draft created
V1.1	23.06.2021	Draft provided for review of CO
V1.2	24.06.2021	Reviewed version by CO requesting minor updates
V1.3	25.06.2021	Finished version including improvements according to review comments

## VALIDATION

Reviewers	Validation date
Work Package Leader	Sebastian Zambal (PRO) 25/06/2021
Coordinator	Leo Schranzhofer (PRO) 25/06/2020

## DOCUMENT DATA

<b>Keywords</b>	Inspection equipment, white light video autofocus, thermography, optical inspection, curing sensor
<b>Point of Contact</b>	Name: Sebastian Zambal Partner: PROFACTOR GmbH Address: Im Stadtgut D1, 4407 Steyr, Austria  Phone: +43 7252 885 254 E-mail: <a href="mailto:sebastian.zambal@profactor.at">sebastian.zambal@profactor.at</a>
<b>Delivery date</b>	25/06/2021

## DISCLAIMER

Any dissemination of results reflects only the authors' view and the European Commission Horizon 2020 is not responsible for any use that may be made of the information Deliverable D4.1 contains.

## Executive Summary

The main purpose of the report is to provide the summary of the inspection equipment deployed in the context of project TINKER. An important goal is to integrate inline process monitoring for different production processes: pick & place, inkjet printing, nano imprint lithography (NIL). These processes pose multiple requirements on inspection and inline monitoring. Sensor technology deployed in TINKER to meet these requirements are comprise optical inspection, thermographic imaging, curing sensor, and thermographic imaging. An overview about this inspection equipment and early tests is provided in this document.

**Introduction part** highlights the main objectives of the Deliverable, which is linked to the corresponding Task and Work Package activities.

**Results and Discussion part** consists of 4 chapters each focusing on one of the specific inspection technologies deployed within the TINKER project.

**Conclusions part** will summarize main conclusion of the performed work, summarizing aspects and performance indicators.

**Outlook and deviations part** will provide an outlook for future activities with respect to DoA and description of deviation, if required.

## Table of Contents

<b>1. Introduction .....</b>	<b>6</b>
1.1. Description of deliverable.....	6
<b>2. Results and Discussion .....</b>	<b>7</b>
2.1. Optical inspection setup .....	7
2.2. White light video autofocus setup .....	10
2.3. Curing sensor setup .....	12
2.4. Thermography setup .....	13
<b>3. Conclusions.....</b>	<b>18</b>
<b>4. Degree of Progress .....</b>	<b>19</b>
<b>5. Outlook and deviation .....</b>	<b>20</b>
<b>6. Appendix.....</b>	<b>21</b>
6.1. Tables Reference .....	21
6.2. Figures Reference .....	21
6.3. Bibliography.....	21

## 1. Introduction

The vision of TINKER is to provide a new cost- effective and resource-efficient pathway for RADAR and LiDAR sensor package fabrication with high throughput up to 250units/min, improved automation by 20%, improved accuracy by 50% and reliability by a factor of 100 to the European automotive and microelectronic industry via additive manufacturing and inline feedback control mechanisms. Autonomous driving and self-driving cars represent one prominent example for the use of microelectronics and sensor, most importantly RADAR and LiDAR sensors. Their respective markets have a big potential, e.g. it is estimated that the market size of LiDAR in automotive will double itself in the next two years (within 2020 to 2022).



Figure 1: TINKER overview

The public awareness and the industrial need for further miniaturization of such sensor packages is the main driver of ongoing efforts in the automotive sector to be able to integrate such devices into the car body like in the bumpers and head lamps instead of attaching them (e.g. on top of the car in case of LiDAR device). Safety (for the driver and others) is the most important key aspect of the automotive sector. Therefore, high-value and high-performance RADAR and LiDAR systems are required for advanced driver-assistance systems (ADAS) as well as robotic cars. Current bottlenecks are the relatively large size of such sensor devices, their weight and power consumption. Since these factors are highly limited within cars, further miniaturization and improving functionality and efficient use of resources is highly demanded.

### 1.1. Description of deliverable

Deliverable D4.1 “Prototype of Inspection Equipment” relates to Task 4.1 in work package 4 “Feedback Control”. The main focus of this task is to set up the relevant inspection equipment and upgrade inspection tools for use in the TINKER project. This includes hardware on the one hand and basic software for read-out of sensor data on the other hand.

## 2. Results and Discussion

The main sensor technologies deployed within the TINKER project are: Optical inspection, white light video autofocus, curing sensors and thermography. Each of these technologies and the respective installations for TINKER are outlined in the following sub-chapters.

### 2.1. Optical inspection setup

Optical inspection is used in the following context:

- Quantification of gaps surrounding bare dies in PCB pockets
- Inspection of the inkjet printing process
- Inspection of nano imprint lithography (NIL) stamp degradation

These different contexts and current inspection equipment are outlined in more detail below.

#### Gap inspection

The camera used for optical inspection of gaps between bare die and PCB has a resolution of 1920 x 1080 pixels. The field of view for the full image is 60 x 34 mm<sup>2</sup>. An example image of bare die inserted into the pocket on the PCB is shown in the figure below.

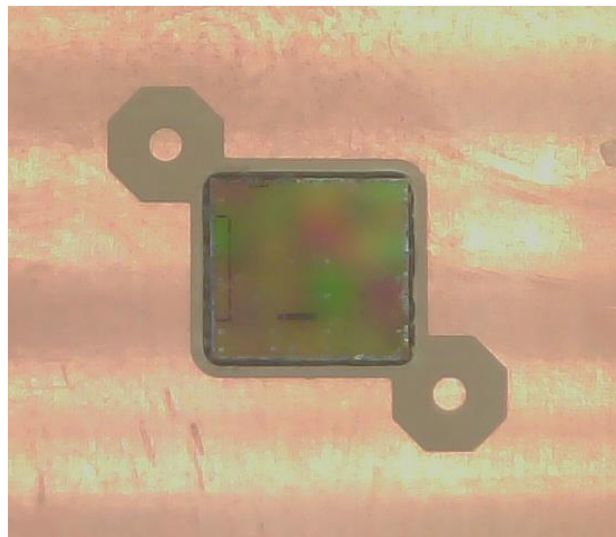


Figure 2: Image acquired for inspection of gap between bare die and PCB (cropped).

#### Inkjet-printing inspection

Optical inspection for inkjet-printing inspection is currently not completed. If possible, cameras will be used that are already available with the respective equipment. The Meyer Burger LP50 printer at PROFACTOR contains an Allied Vision Manta G-032B monochrome camera. This camera supports a maximum resolution of 656 (H) x 492 (V) pixel. With the integrated lens and given working distance, the field of view is approximately 2mm x 1.5mm. By default, the camera is used for marker detection and positioning of printed images. Possibilities to use the camera for inline inspection will be evaluated. In a similar way, the use of existing camera systems for the inkjet printer designed at NOTION will be investigated.

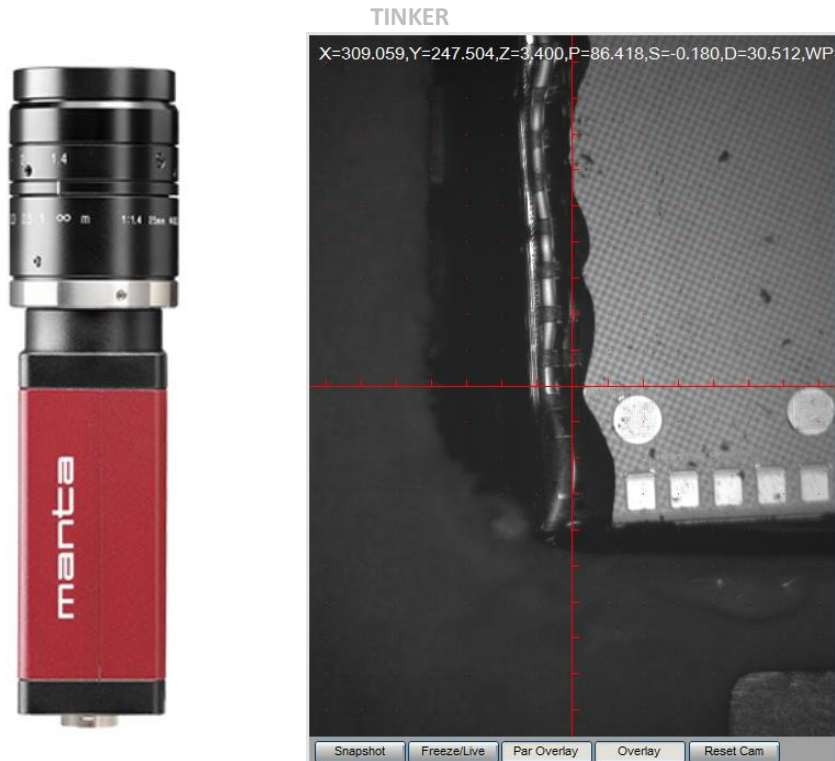


Figure 3: Allied Vision Manta G-032B camera (left) and example image acquired with it showing an image after early experiments with printing to fill up gaps (right).

In case the integrated camera turns out being not suitable for online monitoring at a later stage of the project, integration of additional cameras will be considered. Like the Manta G-032B, additional cameras will have a Gigabit Ethernet (GigE) Vision interface. This is the industry standard for connecting cameras to processing hardware via Ethernet. One possible option is to have additional inspection cameras moving with the print head. In this case, positions of cameras need to be tracked. Another option is to use one or multiple cameras with fixed position. In this case, it might be critical to ensure sufficient resolution. Such a setup, however, would enable fast inspection of larger areas without the need to foresee dedicated motion of the print head that is needed only for inspection.

#### **NIL stamp inspection**

For inspection of NIL stamps, PROFACTORs “soft-NIL stepper” (see also deliverable D5.1) was extended with a dedicated inspection unit. This unit consists of a Dino-Lite microscope camera, a mirror, and an integrated light source. The setup is shown in the figure below.

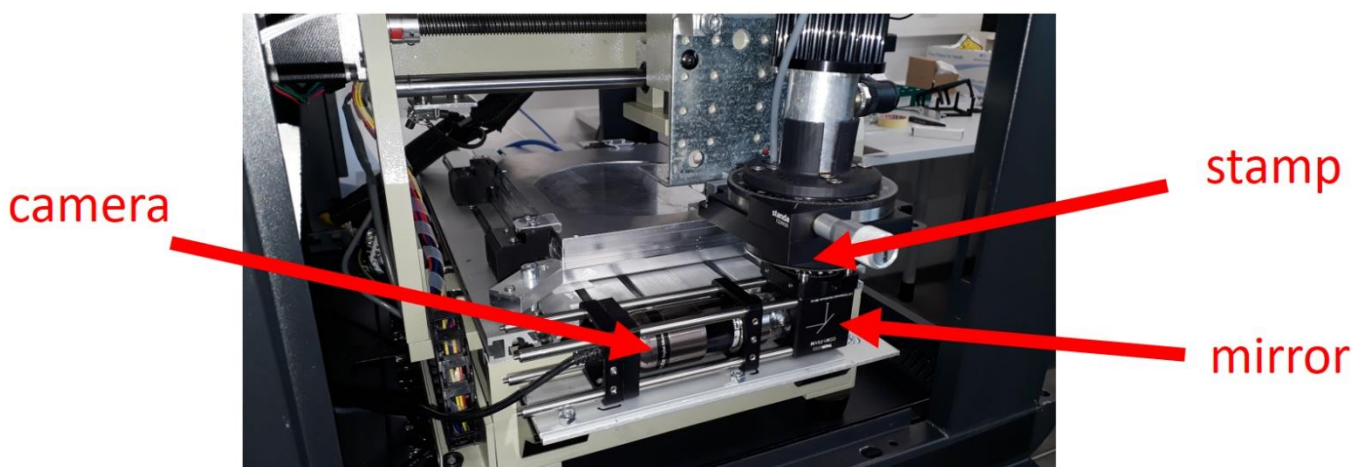


Figure 4: Inspection setup integrated into the soft-NIL stepper at PROFACTOR.



## TINKER

The main goal is to implement automatic inspection of NIL stamp quality. Inspections can be programmed freely. For an inspection, the stepper needs to position the stamp above the inspection unit. The inspection system was developed to allow inspection of the first order diffraction.

The first order diffraction is dependent on the wavelength of the excitation light, the involved incoming and diffraction angle, and the nano-pattern with its orientation in respect to the light. Therefore, the optimal position of the stamp, illumination light source and camera initially need to be set manually. This enables inspection of the first order of diffraction. An example image acquired with the NIL inspection setup is shown in the image below. The advantage of inspecting first order diffraction is the capability of indirectly inspecting wavelength-sized structures with a rather simple setup. As shown in Figure 5, the black dots on the left are defects on the stamp (originating already from the used master) where no nano-pattern is present. In addition to this information, including the intensity of the diffracted light, there is also the information of surface roughness as well as the pattern height. As shown in Figure 6, a narrow band illumination is better suited for the inspection system.

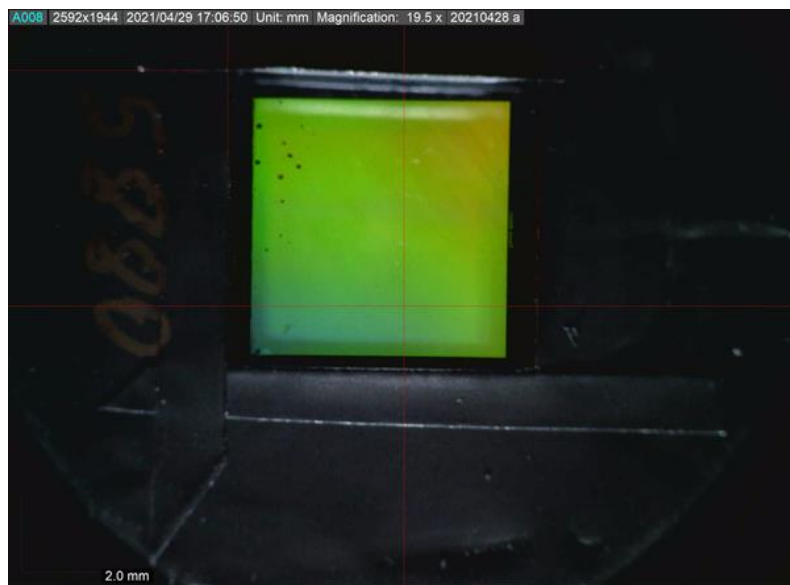


Figure 5: Example image acquired with the NIL inspection unit installed in the Soft-NIL-Stepper at PROFACTOR First order diffraction by using broadband (white-light) excitation (left side) and narrow band excitation (right side).

A typical image analysis result is shown in Figure 6. It shows the original first order diffraction image under narrow band with illumination (a) and a plotted 3D visualization of the intensity (b). By analysing the intensity, areas with lower intensity can be detected automatically. A calculated mask of the image based on the intensity to detect grains, which correspond to areas with no nano-pattern in the image is shown in Figure 6 (c). Some statistical information about the defects can be calculated automatically by using the masking option which is shown in (d). For example, the number of grains can be determined. The next steps towards inline control is an automatic analysis of the images during the imprint process. With this inline inspection, changes on the stamp can be detected early and countermeasures, e.g. cleaning imprints or stamp exchange can be performed. In addition, the possibility of inspecting the surface using a dark field illumination (narrow angle white light illumination) will be determined in the upcoming months. The goal of this is to get additional information about the surface, especially on particle contaminations.

TINKER

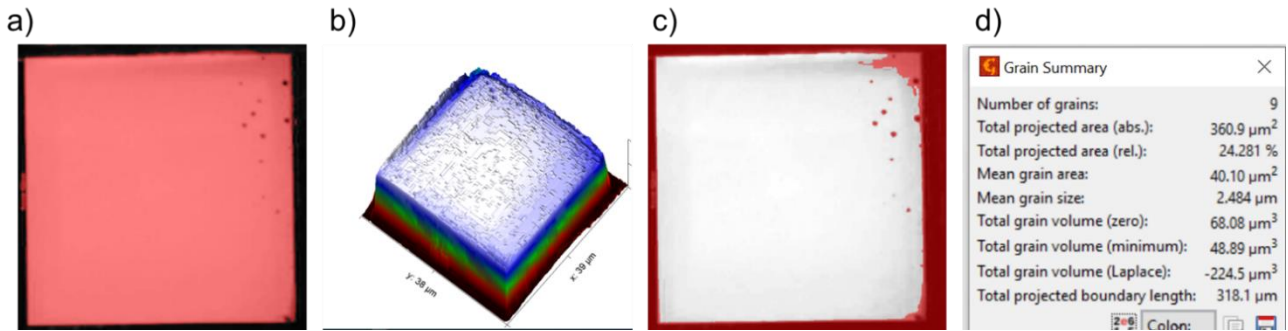


Figure 6: Analysis of a first order diffraction on fresh stamp. Original first order diffraction image under narrow band with illumination (a) and plotted 3D visualization of the intensity (b). Basic masking of the image based on the intensity to detect grains, which correspond to areas with no nano-pattern in the image(c). Some statistical information about the defects by analysing the masked areas (d).

## 2.2. White light video autofocus setup

SENTECH's white-light-autofocus system applies proprietary real-time data analysis in order to measure the height and tilt of multiple points in a certain field-of-view, simultaneously. Moreover, SENTECH's autofocus system will be integrated into BESI's pick-and-place machine (see detailed description of BESI's Pick-and-Place equipment setup in deliverable D3.1). As such SENTECH's autofocus system is evaluated in terms of:

- Verification of the measurement principle
- Measurement accuracy of test samples
- Integration space at BESI's equipment

At first, SENTECH's measurement principle based on a white light video measurement has been evaluated on a mockup daisy chain chip sample provided by INFINEON, see Figure 7. The test wafer consists of several single and differently tilted elements. Moreover, each element exhibits a diffractive character.



Figure 7: Layout of INFINEON's daisy chain chip to evaluate the measurement principle.

As can be seen in Figure 8, a robust signal even on this rough and structured surface can be generated and applied for a reliable autofocus on the sample surface.

## TINKER

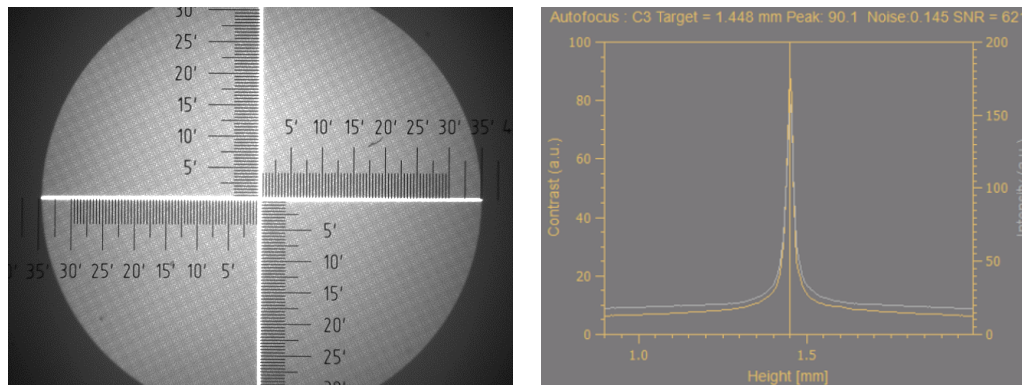


Figure 9: Left: Focus on sample surface. Right: Measurement signal of the autofocus.

Next to the autofocusing of the sample surface, SENTECH's sensor system has the benefit of providing a "single-snap" approach to tilt measurements, even on challenging surface conditions (rough, smooth, shiny, diffractive or diffusive). For a reliable tilt measurement of the daisy chain chips, a system optimization was introduced to get an improved tilt cross for the automated tilt algorithm (see Figure 10)

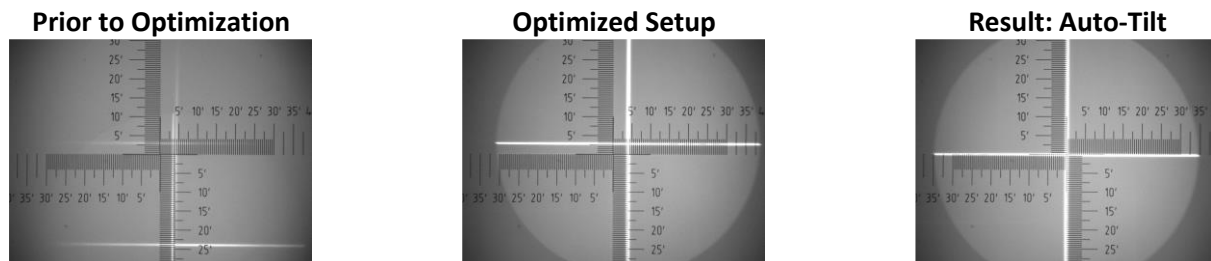


Figure 10: System optimization to improve the tilt measurement capability.

With the successful setup optimization special focus is put on the accuracy of the white-light-autofocus system. Since the system applies a real-time data analysis algorithm to measure height and tilt simultaneously, Table 1 summarizes the accuracy results of the measurement. Exemplarily shown for one daisy chain chip. As a result, the targeted specification of a height accuracy below 3  $\mu\text{m}$  is reached.

Table 1: Accuracy results for height and tilt of the white-light-autofocus system.

	Height [mm]	Tilt y [']	Tilt x [']
	-0.532	12.5	1.7
	-0.531	12.3	1.8
	-0.532	12.4	1.5
	-0.531	12.4	1.8
	-0.529	12.2	1.5
<b>1 <math>\sigma</math></b>	<b>0.0011</b>	<b>0.10</b>	<b>0.14</b>
<b>Target</b>	<b>0.003</b>		

Lastly, in collaboration with BESI, an integration study was carried out to establish SENTECH's white-light-autofocus system into BESI's pick-and-place machine. As can be seen in Figure 11, it is aimed to fit SENTECH's measurement system near the camera of the bondhead assembly. A volume of roughly 20x20x200 mm<sup>3</sup> (grey tube) will be used for the system integration. More details about BESI's bonder can be found in deliverable D3.1.

## TINKER

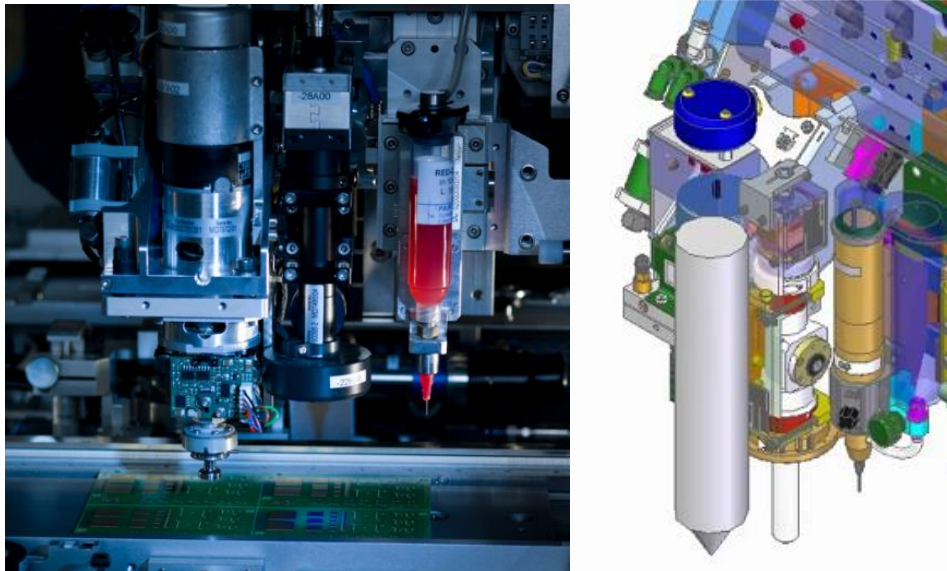


Figure 11: Left: BESL's 2200 evo<sup>plus</sup> modular bondhead assembly allowing the mounting of SENTECH's white-light-autofocus system (grey tube).

### 2.3. Curing sensor setup

The second part of SENTECH is the development of a fast curing sensor. This sensor needs to be designed for the specific resist applied within the TINKER project. The measurement principle is based on following two wavelengths in the mid infrared (MIR) (see Figure 12). As such, the reflectivity measurement is sensitive against the change of the chemical composition, that allows to follow the curing process and moreover to determine the resist before/after curing.

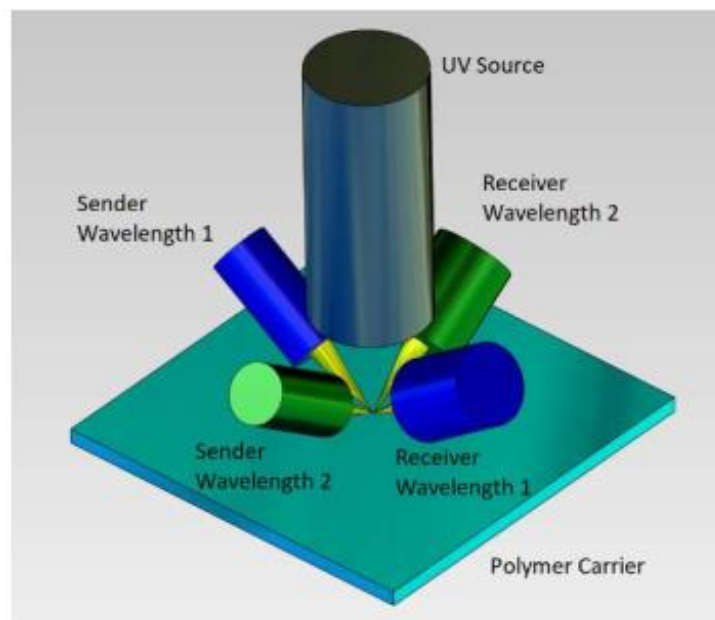


Figure 12: Sketch of the curing sensor setup.

The curing change of the reflectivity spectra in the mid infrared were used in cooperation with PROFACTOR and sensitive wavelength ranges were found. The two-channel design is derived with these data and a sensor prototype with 3D printed components will be provided to PROFACTOR for first tests in a next step.

## 2.4. Thermography setup

Thermography is used to inspect the conductivity of inkjet-printed conductive paths. In case of good conductivity, there must be a good thermal connection too. Therefore, periodic laser excitation close to the conductive path at the PCB-board should result in a thermal signal at the other end of the conductive path, i.e. at chip-side. The chip-side signal is shifted in its phase. This method is called pulse phase thermography or lock-in thermography [1]. The evaluation of the thermal signal is analysed in order to assess the quality of the conductive path.

A laser is programmed to emit pulses. The testing sample is located at the focal distance from its beam exit to form a small spot at the copper surface of the testing sample. This is observed by a thermal camera. The direction of view is not perpendicular to the surface in order to avoid the self-reflection. The following figures show the schematic setup for thermographic inspection and images of the current setup.

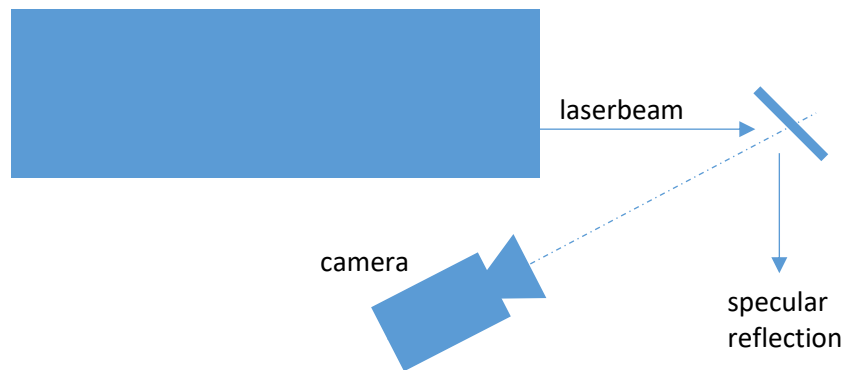


Figure 13: Sketch of thermographic inspection setup with sample, camera, and laser (top view).



Figure 14: Photograph of testrig with laser, camera, and test sample.

The laser unit is equipped with a deflection system to control the direction, in which the laser beam is emitted. This deflection can be programmed to move the laser spot. However, it is currently just used for fine tuning of the laser position which does not change during the inspection. Details about Camera and Laser are listed below in Table 2.



Table 2: Thermography test setup specifications at PROFACTOR

Camera	Laser
Infratec ImageIR 8300 (640x512, InSb, f=50mm)	CO <sub>2</sub> -Laser, P=100W (nominal power)
texp=473μs	Set to 10% of nominal power (pulse with modulation)
framerate=1kHz	Set to 25kHz pulse width frequency
AOI=quarter image, centered	Heating duration of each spot is set to 10ms, 50ms and 200ms
spatial resolution = 105μm per pixel	Set to alternating spots separated by 3mm distance (period is twice the heating duration). Each spot is heating up and cooling down for the same duration. The 2nd spot is not used in evaluation. It is heating while the 1st spot is cooling down. This method enables constant laser power

A first set of trials was performed for inkjet-printed conductive paths. Microscope images of two initial samples are shown below. The images show the bare dies placed into pockets of printed circuit boards. Conductive paths with 80 μm width were inkjet-printed across the gap between PCB and bare die. Four individual conductive paths were printed for each bare die: across each of the four edges of the bare die.

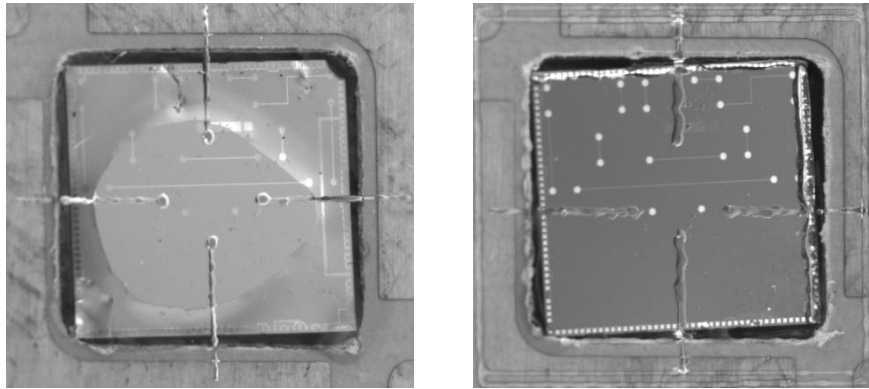


Figure 15: Two different bare dies inserted into cavities on a PCB. Conductive paths are added via inkjet printing across all edges of each bare die.

For initial thermography experiments, the spatial resolution of acquired images was 105 μm per pixel. The spot diameter at half of the maximum amplitude was 840 μm.

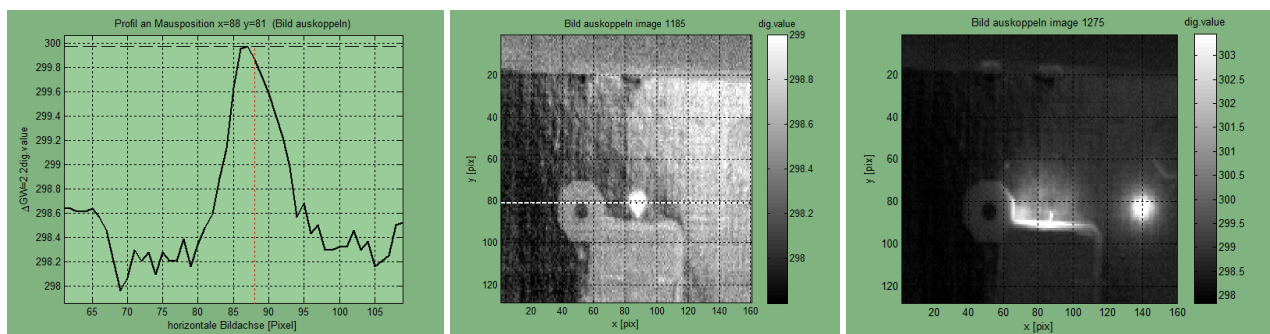


Figure 16: Laser spot profile (left) and spot location (middle) and 2<sup>nd</sup> spot (right).

TINKER

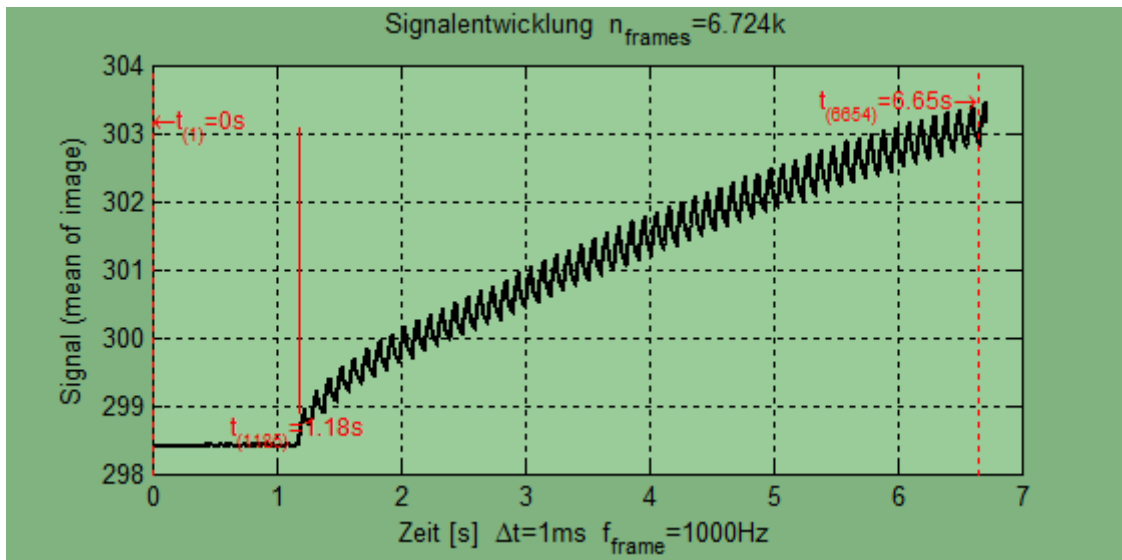


Figure 17: Overview of timing for manually triggered test (example with 50ms heating duration)

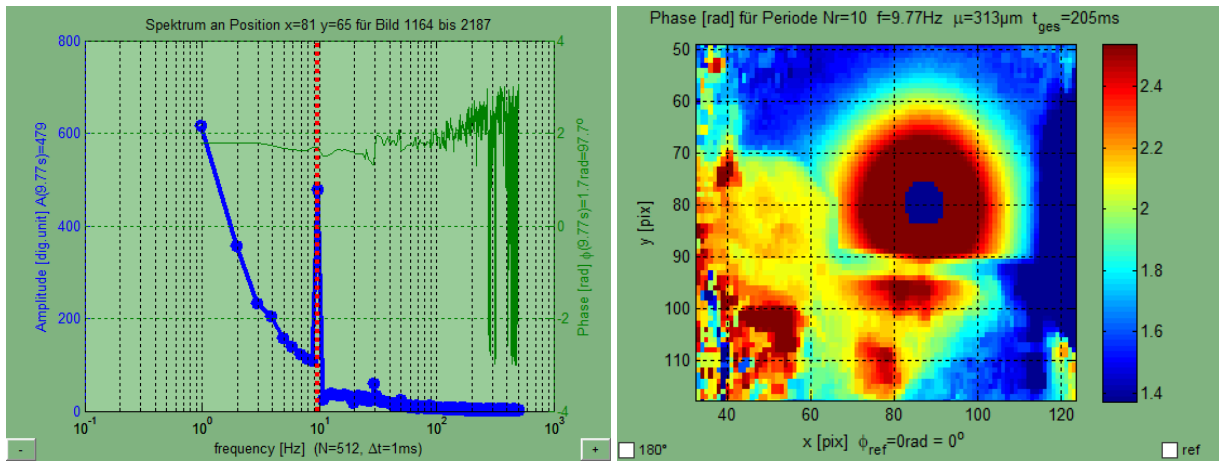
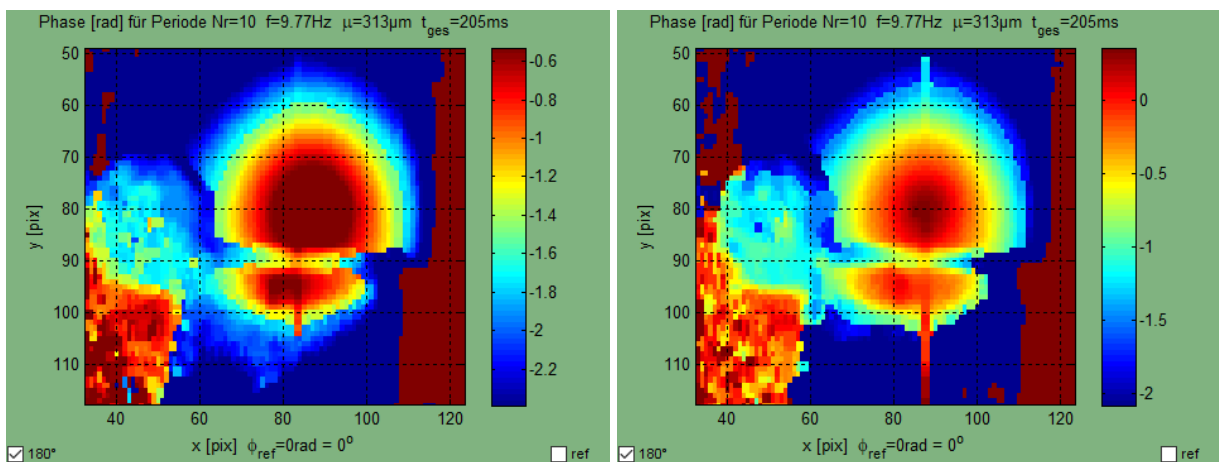
Figure 18: Spectrum of the thermal signal (left) and phase image for  $\sim 10\text{Hz}$  (right) for spot heating duration is 50ms.

Figure 19: Same as above, but spot closer to chip.

## TINKER

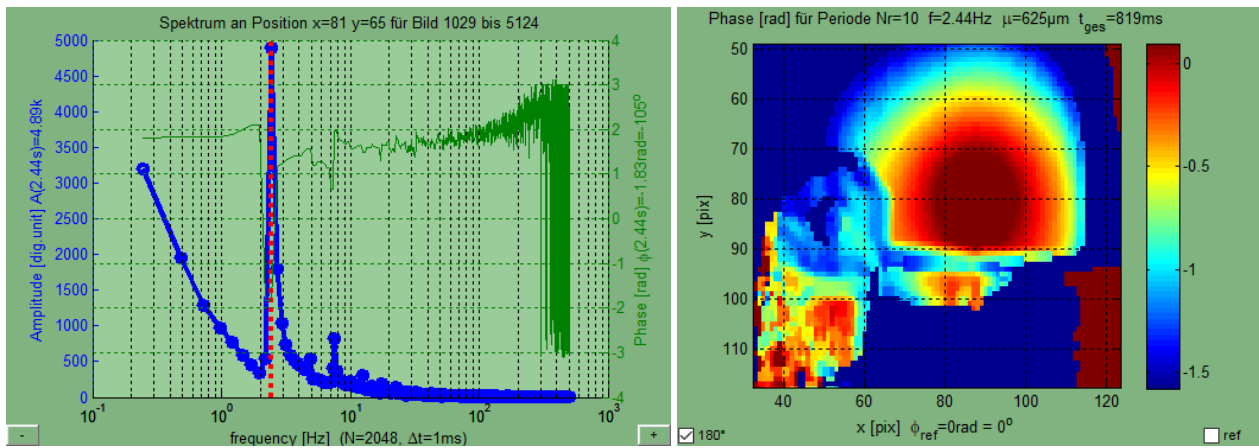


Figure 20: Spectrum (left) and phase image for 2.5Hz for spot heating duration is 200ms.

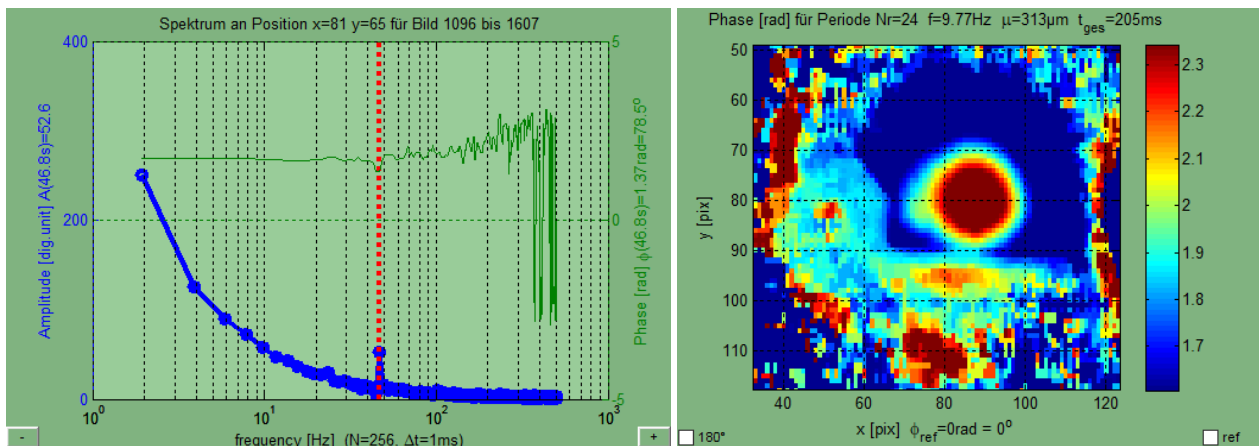


Figure 21: Spectrum (left) and phase image for 50Hz for spot heating duration is 10ms.

Approximation of thermal reaction:

Based on Dirak pulse at spot:  $\kappa = \frac{r^2}{6t}$   $\left| \begin{array}{l} r..distance\ from\ spot \\ t..time,\ when\ (T(r)=T(r,max)) \Rightarrow t = \frac{r^2}{6\kappa} \\ \kappa..thermal\ diffusivity \end{array} \right.$

Table 3: Material properties of Cu

Property	Value	Unit
Conductivity	386	W/m/K
Density	8.95	mg/m <sup>3</sup>
Thermal capacity	383	J/kg/K
Thermal diffusivity	113	μ(m <sup>2</sup> /s)
Thermal effusivity	36.4	kJ/(Km <sup>2</sup> sqrt(s))

The temperature  $T(r)$  after a Dirac pulse at the spot ( $r=0$ ) with distance  $r$  from the spot is investigated. The temperature reaches a maximum at time  $t$  after the excitation pulse with

- $t=1.5ms$  for  $r = 1mm$
- $t=5.9ms$  for  $r=2mm$  and
- $t=13.3ms$  for  $r=3mm$ .

Consequently, it takes at least time  $t$  for the (significant amount of) heat to be conducted along a path of  $r$ . This approximation is just to make sure, that a thermal reaction  $r$  away from the spot is contained in the thermal signal, if the duration of observation is equal or larger than  $t$ .



## TINKER

Since the thermal signal condition is poor in these first tests, it is hard to find the proper setup. Especially the lock-in frequency must be set to a value, to maximize the phase contrast in the phase images. Therefore it is planned, to simulate heat conduction with different frequencies for laser excitation (which is the same as the lock-in frequency). By evaluation of the simulated results, the frequency can be optimized and adjusted for improvement and further tests.

As a first guess, based on the first phase images, a lock-in frequency of approximately 50Hz seems to deliver good results. The signal condition is relatively poor, and doesn't allow direct comparison of the phase amplitudes. Simulation is free of distortions, as occurring in the real thermal images. It therefore should be the proper tool to prove that there is a phase signal difference between good and bad connections. Further investigations will be conducted in order to retrieve the resolution that is necessary for classification.

### 3. Conclusions

The TINKER project aims to improve inline monitoring and feedback control with multiple sensor technologies and for different process stages. The initial setup for inspection technologies is outlined in this document. So far, installations are at an early stage. The basic functionality and basic principles could be demonstrated. An early test sample of PCB with pocket, bare die, and inkjet-printed supported initial development of inspection systems. As further samples become available and systems evolve over the course of the project, inspection systems will be improved in parallel developments.

#### **4. Degree of Progress**

All inspection technologies targeted by TINKER were demonstrated as prototypes. In this sense, all building blocks for the present deliverable are in place. In the context of individual processes, it might be necessary to extend or modify the current inspection setups. This will become clearer as more inspection tests are performed. For example, it might be necessary to integrate new/additional cameras for inkjet printing. However, there will only be minor changes that can be done very quickly.

## 5. Outlook and deviation

Upcoming activities will include the execution of additional experiments. Conclusions drawn from these will enable the improvement of inspection technologies. Furthermore, evaluation software will be improved to derive high-level information from acquired data and to derive the required control actions.

## 6. Appendix

### 6.1. Tables Reference

Table 1: Accuracy results for height and tilt of the white-light-autofocus system. ....	11
Table 2: Thermography test setup specifications at PROFACTOR.....	14

### 6.2. Figures Reference

Figure 1: TINKER overview .....	6
Figure 2: Image acquired for inspection of gap between bare die and PCB (cropped). ....	7
Figure 3: Allied Vision Manta G-032B camera (left) and example image acquired with it showing an image after early experiments with printing to fill up gaps (right).....	8
Figure 4: Inspection setup integrated into the soft-NIL stepper at PROFACTOR. ....	8
Figure 5: Example image acquired with the NIL inspection unit installed in the Soft-NIL-Stepper at PROFACTOR First order diffraction by using broadband (white-light) excitation (left side) and narrow band excitation (right side). ...	9
Figure 6 Analysis of a first order diffraction on fresh stamp. Original first order diffraction image under narrow band with illumination (a) and plotted 3D visualization of the intensity (b). Basic masking of the image based on the intensity to detect grains, which correspond to areas with no nano-pattern in the image(c). Some statistical information about the defects by analysing the masked areas (d).....	10
Figure 7: Layout of INFINEON's daisy chain chip to evaluate the measurement principle. ....	10
As can be seen in Figure 8, a robust signal even on this rough and structured surface can be generated and applied for a reliable autofocus on the sample surface. ....	10
Figure 9: Left: Focus on sample surface. Right: Measurement signal of the autofocus. ....	11
Figure 10: System optimization to improve the tilt measurement capability.....	11
Figure 11: Left: BESI's 2200 evo <sup>plus</sup> modular bondhead assembly allowing the mounting of SENTECH's white-light-autofocus system (grey tube). ....	12
Figure 12: Sketch of the curing sensor setup. ....	12
Figure 13: Sketch of thermographic inspection setup with sample, camera, and laser (top view). ....	13
Figure 14: Photograph of testrig with laser, camera, and test sample. ....	13
Figure 15: Two different bare dies inserted into cavities on a PCB. Conductive paths are added via inkjet printing across all edges of each bare die. ....	14
Figure 16: Laser spot profile (left) and spot location (middle) and 2 <sup>nd</sup> spot (right). ....	14
Figure 17: Overview of timing for manually triggered test (example with 50ms heating duration) ....	15
Figure 18: Spectrum of the thermal signal (left) and phase image for ~10Hz (right) for spot heating duration is 50ms. ....	15
Figure 19: Same as above, but spot closer to chip. ....	15
Figure 20: Spectrum (left) and phase image for 2.5Hz for spot heating duration is 200ms. ....	16
Figure 21: Spectrum (left) and phase image for 50Hz for spot heating duration is 10ms. ....	16

### 6.3. Bibliography

- [1] Mathias Ziegler, Erik Thiel and Samim Ahmadi, Lock-in Thermography using High Power Laser Sources, 12th European Conference on Non-Destructive Testing (ECNDT 2018), Gothenburg 2018, June 11-15 (ECNDT 2018)